The Study of Transition from Elastohydrodynamic to Mixed and Boundary Lubrication

Dong Zhu
Eaton Corporation
26201 Northwestern Highway
Southfield, Michigan 48037, U.S.A.

And

Yuan-Zhong Hu
State Key Laboratory of Tribology
Tsinghua University
Beijing 100084, China

A unified numerical approach for point contact problems is presented in this paper, simulating various lubrication conditions that cover the entire transition from full film elastohydrodynamic, mixed, down to boundary lubrication (or dry contact). As is known, the commonly used method to solve the EHL problem is to employ the Reynolds Equation coupled with the elasticity equation. However, when the lubricant film is very thin, finding a convergent solution becomes difficult and possible asperity contact may cause severe computation overflow. Also, for mixed lubrication the boundary of hydrodynamic region may momentarily change its irregular shape and location. The boundary condition of the Reynolds Equation is therefore difficult to handle when the conventional solution method is used. The present approach is based on the idea that the same Reynolds Equation may be used for both the hydrodynamic region and the contact region. Under the constraint of zero film thickness, the Reynolds Equation is reduced to a simple form equivalent to the expression of dry contact problem. With this reduced Reynolds Equation the numerical procedure can be unified for both the hydrodynamic and contact regions, and the solution method is simple and robust. A series of sample cases have been analyzed for both smooth surfaces and real machined surfaces with 3-dimensional roughness. These cases cover the entire transition from the full film EHL (rolling speed as high as U=15000 mm/s) down to the boundary lubrication at U=0.001 mm/s. So far no convergence problem has been encountered even for l ratios lower than 0.03. Typical results for average film thickness/gap and contact area ratio vs. rolling speed are also presented for the entire continuous transition.

KEY WORDS

Mixed Lubrication, Elastohydrodynamic Lubrication (EHL), Boundary Lubrication, Contact Analysis, Surface Roughness Effect

INTRODUCTION

In engineering practice, most oil- or grease-lubricated mechanical components transmitting power/motion with concentrated contacts, such as gears, rolling element bearings, cams and traction drives, usually operate in the mixed or boundary lubrication regions. Surface roughness heights are typically of the same order as, or one order of magnitude greater than, the average lubricant film thickness. Therefore, the applied load is usually shared by both hydrodynamic lubricant film and asperity contacts caused by the surface roughness. A good lubrication design should maximize the probability of having contacting surfaces separated by the hydrodynamic lubricant film. On the other hand, most surface failures, such as excessive wear, pitting due to contact fatigue and scuffing, are directly related to severe asperity contacts and lubrication breakdown. In order to better understand lubrication mechanism and improve component design/performance/reliability, it is essential to study the roughness effect on the lubrication, and investigate the transition from the full film EHL to the mixed and boundary lubrication.

Great efforts have been made in the last 20-30 years to try to understand the mechanism of mixed lubrication. Since it is difficult to experimentally measure the film thickness (or gap) when the two surfaces are rough with asperity contacts, researchers have to rely more on the analytical / numerical study. There have been two main

Nomenclature

a	= radius of Hertzian contact circle
A_c	= contact area ratio
E'	= effective Young's modulus
G^*	= aE', dimensionless material parameter
h	= local film thickness (or gap)
h_a	= average central film thickness
p	= hydrodynamic pressure, or pressure in general
p_c	= asperity contact pressure
p_h	= maximum Hertzian pressure
R_q	= root mean square (RMS) surface roughness
R_x	= effective radius in x-z plane
R_y	= effective radius in y-z plane
S	= $(u_2 - u_1)/U$, slide-to-roll ratio
T	= tU/a, dimensionless time
t	= time
U^*	= $h_oU/(E'R_x)$, dimensionless speed parameter
U	= $(u_1 + u_2)/2$, rolling velocity
u_1, u_2	= velocities of surface 1 and surface 2
V	= surface deformation
W^*	= $w/(E'R_x^2)$, dimensionless load parameter
w	= load
W_c	= contact load ratio
X	= x/a
x	= x-coordinate (rolling direction)
Y	= y/a
y	= y-coordinate
a	= pressure-viscosity exponent
d_1,d_2	= roughness heights for surfaces 1 and 2
h	= viscosity
h_o	= viscosity under ambient condition
h^*	= effective viscosity
λ	= h_a/s, film thickness ratio
r	= density
r_o	= density under ambient condition
s	= $(R_{q1}^2 + R_{q2}^2)^{0.5}$, composite RMS roughness

types of numerical analysis available. The first type includes stochastic models that use selected statistic parameters to represent random characteristics of rough surface lubrication. Early models were developed by Christensen (1), Elrod (2), Tonder (3), and Patir and Cheng (4) et al. Among these models, the one by Patir and Cheng has been widely accepted and helpful for basic understanding of roughness effect on lubrication. It has provided a simplified tool for estimating the film thickness based on the surface roughness and its orientation. A typical mixed EHL analysis for the point contact problem, using Patir and Cheng's average fluid model, was presented by Zhu and Cheng (5), in which hydrodynamic and contact pressure were separately calculated and then simply superimposed to balance the applied load. This type of stochastic analysis, however, deals only with the global effect of surface topography. It provides no detailed information about local pressure peaks, local film thickness fluctuations and asperity deformation, which are usually critical for the study of lubrication breakdown and surface failure. Also, since the rough surface lubrication is so complicated, after many years of effort researchers tend to believe that it is probably impossible to describe its characteristics satisfactorily with only a simple mathematical expression and a small number of stochastic parameters.

Recently, as computer technology is better developed, more attention has been given to the second type of analysis — deterministic models. This type of analysis uses simplified or real surface geometric profiles as inputs of the numerical solution, so statistic parameters are no longer needed. The real surface topography, however, is usually very complicated, and the problem may become strongly time-dependent due to deformed moving surface asperities. Therefore, satisfactory deterministic solutions are difficult to find, requiring considerably more computational power and better surface analysis capability.

Available steady state deterministic models for point contact problems include those by Lubrecht, ten Napel and Bosma (6), Kweh, Evans and Snidle, et al (7,8), and Ai and Cheng (9). In these models the rough surface is stationary and the moving surface is perfectly smooth, so the solution is time-independent. Since steady state models are not satisfactory for most engineering applications, transient solutions with at least one moving rough surface have been developed. Available transient models include those by Ai, Cheng and Zheng (10,11), Venner and Lubrecht (12), Xu and Sadeghi (13), and Zhu and Ai (14). Most models mentioned above used artificial or simplified surface asperities (e.g. semi-spherical bumps or sinusoidal waves) that pass through the otherwise perfectly smooth EHL conjunction, except those in (13) and (14). Xu and Sadeghi's model (13) was probably the first one using a 3-dimensional measured rough surface for point contact EHL. It seems, however, that the two sample surfaces used in their paper were still very smooth. The mean roughness were 0.0023 and 0.0334 μm respectively, below the typical range for most engineering surfaces.

Optically measured 3-dimensional rough surfaces made by common machining processes, such as turning, grinding, honing, and shaving, have been used by Zhu and Ai (14) in their full numerical solution to the point contact EHL. With their model, the surface roughness can be in a practical range from 0.1 to 1.0 μm, as long as there is still a significant lubricant film. Both contacting surfaces can be rough and moving at different velocities. The transient solution is obtained by using a multi-grid scheme. Even though this model seems to be relatively more capable, generally it can only handle full film lubrication with no heavy asperity contact. Actually, all of the available models mentioned above do not seem to be able to handle the real mixed lubrication and the transition to boundary lubrication. Basically, two major problems still remain unsolved as described below.

First, all of the available solution methods seem to have convergence problems when the lubricant film becomes very thin. Please note that for the mixed lubrication study based on deterministic models, the conventional definition of "central film thickness" needs to be modified. In the present work it is replaced with "average film thickness" (or "average gap") defined by Zhu and Ai (14) in order to better describe the global lubrication characteristics consistently under different lubrication conditions. According to their definition, the average film thickness, h_a, is calculated within a certain radius from the center of normalized Hertzian contact zone. This radius equals 2/3 of the Hertzian radius, so that a sufficient number of data points can be included in the calculation, but the possible edge effect can be avoided. Also, the commonly used term "film thickness ratio" or "λ ratio" needs to be clarified in order to avoid confusion. In the present study it is defined as the ratio of average film thickness to the composite roughness, $\lambda=h_a/\sigma$. It is believed, based on the published results, that most available models mentioned above can only handle cases at λ ratios above 3.0. Some models, such as the one by Zhu and Ai, may be able to get down to 2.5 and very occasionally to 2.0-2.2. However, this is not even close to the real mixed lubrication, in which the λ ratio could be in a range of 0.3-1.0 or lower. The problem appears to be that the numerical solution may not converge when the operating condition is severe and the lubricant film is thin. Possible asperity contacts may often cause computation overflow.

Secondly, for the mixed lubrication the entire solution domain is divided into two different regions — the hydrodynamic region where the two surfaces are separated by the lubricant film, and the contact region where the surfaces are in contact and the lubricant flow is blocked. When the rough surfaces are moving with the asperities in contact, there could be many contact areas and the boundary of hydrodynamic region may momentarily change its irregular shape and location. The pressure at the boundary is most likely unknown. The boundary condition of Reynolds Equation, therefore, is very difficult to handle when the conventional solution method is used. That is probably the main reason why no successful deterministic solution to the mixed lubrication has been published until most recently. In July, 1999, Jiang, Hua, Cheng, Ai and Lee (15) published their numerical model for the mixed lubrication, which for the first time solves for hydrodynamic and asperity contact pressure simultaneously. In their analysis, 3-dimensional rough surface profile is used and the Reynolds Equation is solved with the multi-grid scheme. The FFT procedure is utilized to calculate the surface deformation and the asperity contact pressure. In an iterative procedure the actual contact pressure at the borders of asperity contact areas is used as the boundary condition of Reynolds Equation for the hydrodynamic region. A typical case, using a 3-dimensional measured rough surface, is presented, in which a converged solution at a λ ratio of 1.16 and an asperity contact area ratio of 12% is achieved. This model appears to be a significant advancement for the mixed lubrication study. However, more efforts are still needed in order to solve cases at lower λ ratios and study the entire transition from the full film down to mixed and boundary lubrication.

This paper presents a new numerical approach that is capable of simulating various lubrication conditions covering the entire transition from the full film elastohydrodynamic, mixed, down to boundary lubrication (or dry contact). The developed model is based on the idea that the same Reynolds Equation can be used for both the hydrodynamic and the contact regions. Under the constraint of zero film thickness, the Reynolds Equation is reduced to a simple form equivalent to the expression of dry contact problem. With this reduced Reynolds Equation the numerical procedure can be unified for both regions, and the solution method is simple and robust. A series of sample cases have been analyzed for both smooth surfaces and real machined surfaces with 3-dimensional roughness. These cases cover the entire transition from the full film EHL (rolling speed as high as U=15000 mm/s) down to the boundary lubrication at U=0.001 mm/s. So far no convergence problem has been encountered even at λ ratios lower than 0.03. Typical results for average film thickness and contact area ratio vs. rolling speed are also presented for the entire transition.

A NEW APPROACH FOR MIXED LUBRICATION

As is well known, in the hydrodynamic region, the pressure is governed by the Reynolds Equation that can be expressed as

$$\frac{\partial}{\partial x}\left(\frac{\rho}{12\eta^*}h^3\frac{\partial p}{\partial x}\right)+\frac{\partial}{\partial y}\left(\frac{\rho}{12\eta^*}h^3\frac{\partial p}{\partial y}\right)=U\frac{\partial(\rho h)}{\partial x}+\frac{\partial(\rho h)}{\partial t} \quad [1]$$

When solving this equation pressure p should be given at the border of solution domain as a boundary condition, while the cavitation condition should also be satisfied. The x-coordinate is chosen to coincide with the rolling direction. Lubricant properties, effective viscosity η^* and density ρ, will be discussed later in this section. The local lubricant film thickness (or gap) is calculated by:

$$h = h_0(t) + B_x x^2 + B_y y^2 + V(x,y,t) + d_1(x,y,t) + d_2(x,y,t) \quad [2]$$

where B_x and B_y are constants related to the original geometry of contacting bodies, δ_1 and δ_2 denote the roughness amplitudes of surface 1 and 2 respectively, and V is the surface deformation calculated by

$$V(x,y,t)=\frac{2}{\pi E'}\iint_{\Omega}\frac{p(\xi,\varsigma)+p_c(\xi,\varsigma)}{\sqrt{(x-\xi)^2+(y-\varsigma)^2}}d\xi d\varsigma \quad [3]$$

where p is the hydrodynamic pressure and p_c asperity contact pressure. The hydrodynamic pressure can be determined by solving the coupled Equations [1], [2] and [3] in the hydrodynamic region. However, conventional solution methods require the knowledge of border position and boundary condition between the hydrodynamic and contact regions. It is quite difficult to collect such information, because the asperity contacts may produce many contact regions with irregular and time-dependent contours.

The new approach employed in the present study is to use the same Reynolds Equation consistently in both the hydrodynamic and contact regions. The idea is based on the belief that the solution of Reynolds Equation under the constraint of h= 0 will give the same result as that from the contact equation.

The physical interpretation of Reynolds Equation [1] is a balance of fluid flow. The left-hand side of the equation represents the lubricant flow due to the hydrodynamic pressure, while the two terms on the right-hand side stand for the lubricant flow caused by surface motion in both the tangential and normal directions. When the film thickness hits zero, the pressure flow vanishes, and the Reynolds Equation is reduced to the following form:

$$U\frac{\partial h}{\partial x}+\frac{\partial h}{\partial t}=0 \qquad at \quad h=0 \quad [4]$$

Please note that at the border between the hydrodynamic and contact regions we have h=0 but $\P h/\P x$ and $\P h/\P t$ may not be zero. Within the contact regions, however, it is reasonable to subsequently turn off the squeeze term in Equation [4]. This will lead to a further reduced equation as follows:

$$\frac{\partial h}{\partial x}=0 \qquad \text{(Within contact regions where } h=\frac{\P h}{\P t}=0\text{)} \quad [5]$$

Substituting Equation [2] into Equation [5] yields

$$2B_x x+\frac{\partial V}{\partial x}+\frac{\partial \delta_1}{\partial x}+\frac{\partial \delta_2}{\partial x}=0 \qquad \text{(Where } h=\frac{\P h}{\P t}=0\text{)} \quad [6]$$

It can be seen from the above discussion that, as Equations [4] and [5] are actually special cases of Equation [1], a unified equation system and numerical scheme can be applied to both the hydrodynamic and contact areas. A full numerical solution over the entire computation domain can thus be obtained by solving one equation system. In this way both hydrodynamic and contact pressure can be obtained through the same iteration loop without requiring any information about the contact borders and boundary conditions between the hydrodynamic and contact regions. More importantly, this approach has been proven to be successful in computation practice to reach convergent solutions under very severe operating conditions. More than 100 cases have been analyzed, and so far no convergence problem has been encountered even for those at λ ratios as low as 0.02-0.03 at rolling speeds as low as 0.001 mm/s (which can practically be considered as stationary).

An effective viscosity η^* has been introduced in Equation [1] to describe the non-Newtonian lubricant properties. Assuming the variation of viscosity along the z-direction (across the film thickness) can be ignored, one can calculate effective viscosity η^* as follows considering possible shear-thinning effect (Please see Yang and Wen (16) for more details):

$$\frac{1}{\eta^*}=\frac{1}{\eta}\frac{\tau_0}{\tau_1}\mathrm{Sinh}\left(\frac{\tau_1}{\tau_0}\right) \quad [7]$$

where τ_0 is a reference shear stress. Its value has been given as τ_0=18.0 MPa in this paper for a typical mineral oil. τ_1 denotes the shear stress acting on the lower surface (Surface 1), and η is the limiting viscosity at low shear rate, which is assumed to be a function of pressure, following the Barus law:

$$\eta=\eta_0\exp(\alpha p) \quad [8]$$

The density of lubricant is also dependent on pressure, given by:

$$\rho=\rho_0\left(1+\frac{0.6\times10^{-9}p}{1+1.7\times10^{-9}p}\right) \quad [9]$$

NUMERICAL PROCEDURE

The discretization of the equations and the relaxation iterative scheme are similar to those described in detail by Ai (17) and others, but modifications are made to turn off the pressure flow and squeeze terms in the asperity contact areas, as explained in the last section.

First, when solving the Reynolds Equation with the iterative procedure, a very small value, ε_1=0.000001, is used as a criterion for checking if h=0. If dimensionless film thickness, H=h/a, falls below ε_1, it is considered that the film thickness is practically zero, the two surfaces are in contact and the pressure flow term in the Reynolds Equation should be turned off. In the same way, another small value, ε_2=0.00001, is used for checking $\P h/\P x$. If both H$\le\varepsilon_1$ and $\P h/\P x \le \varepsilon_2$ are found at the same time, it is inside the contact area and the squeeze term should also be removed. In other words, different equations will be chosen based on different H and $\P h/\P x$ values:

Use Equation [1]	when $H > \varepsilon_1$
Use Equation [4]	when $H \le \varepsilon_1$ but $\P h/\P x > \varepsilon_2$
Use Equation [5]	when $H \le \varepsilon_1$ and $\P h/\P x \le \varepsilon_2$

All of the selected equations will be solved in the same way within the same iteration loop. Since both the hydrodynamic and contact pressure are obtained from the same equation system and the same iterative procedure, from now on, the symbol p will be used for pressure in general, which could be the hydrodynamic pressure when $H>\varepsilon_1$, or the contact pressure if $H \le \varepsilon_1$.

In order to speed up the calculation of surface deformation, a multi-level integration technique is implemented in the present study. The solution domain is determined as $-1.9 \le X \le 1.1$ and $-1.5 \le Y \le 1.5$. The computational grid covering the domain consists of 257*257 nodes equally spaced. This corresponds to a spatial mesh size of $\Delta X = \Delta Y = 0.0117$, which is considerably smaller than those used by Ai and Cheng (9)(17), Venner and Lubrecht (12), and Xu and Sadeghi (13), et al., but slightly larger than that by Jiang, Hua, and Cheng, et al. (about 0.0093)(15). The numerical solution of the corresponding smooth surface case is pre-calculated under the same operating conditions, and then employed as an initial value of the transient rough surface case. From the given initial value the computation proceeds with a time step length of ΔT= 0.015 for artificial asperities, or 0.0075 for measured 3-dimensional roughness.

RESULTS AND DISCUSSIONS

In order to investigate the transition from the full film EHL to the mixed and boundary lubrication, a series of cases have been chosen

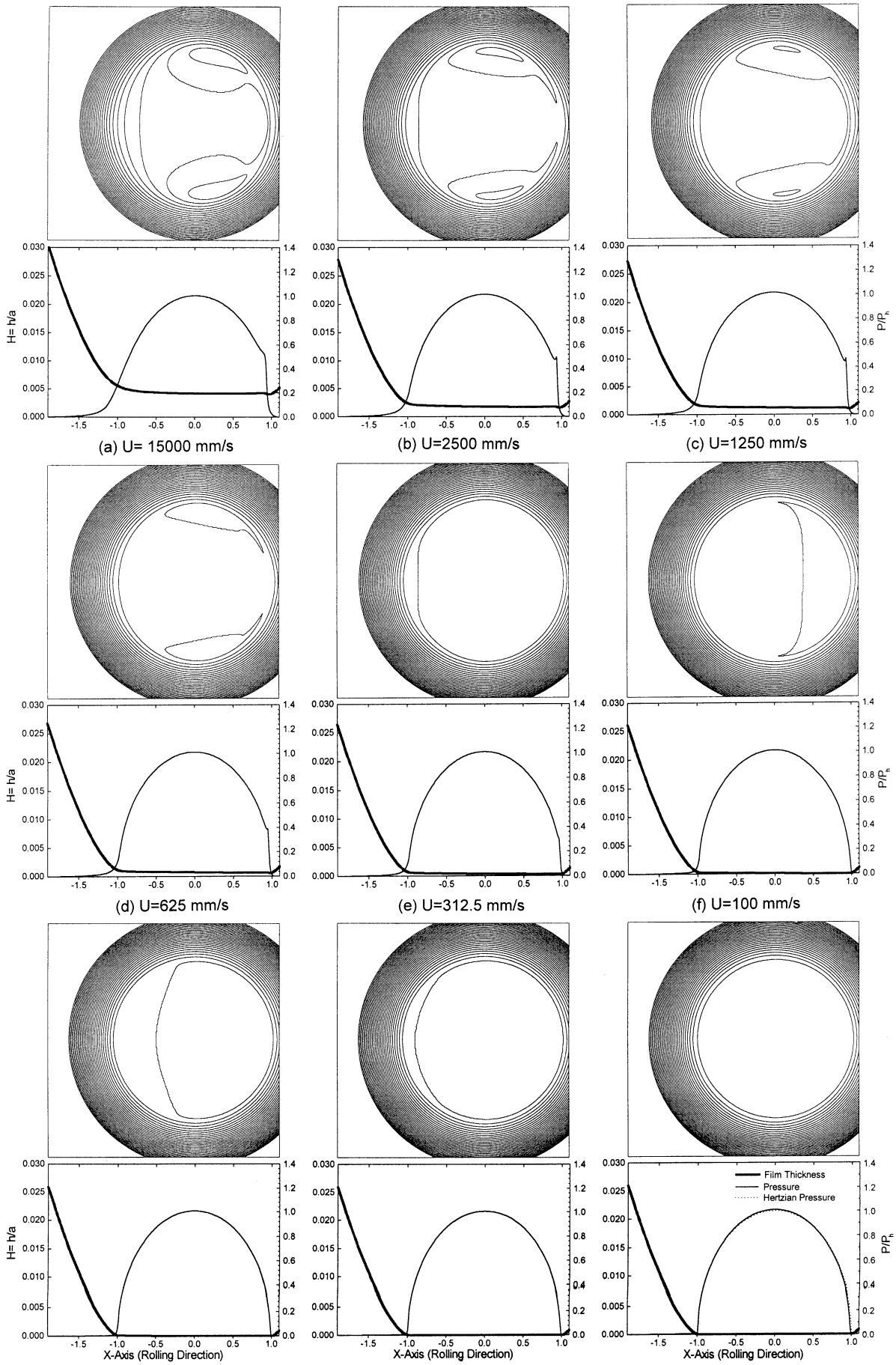

(a) U= 15000 mm/s (b) U=2500 mm/s (c) U=1250 mm/s

(d) U=625 mm/s (e) U=312.5 mm/s (f) U=100 mm/s

(g) U=30 mm/s (h) U=5 mm/s (i) U=0.001 mm/s

Figure 1

with two types of surface roughness in a very wide range of rolling speed, but otherwise under the same operating conditions. The applied load is fixed at w=800 N, the material properties are E'=219.78 GPa, η_o=0.096 Pa.s, and α=18.2 GPa $^{-1}$. The geometric parameters are $R_x = R_y$ =19.05 mm, so that the Hertzian contact zone is a circular area of 0.4725 mm in radius, and the maximum Hertzian pressure is P_h= 1.711 GPa. The rolling velocity is changed from U= 0.001 up to 15000 mm/s, so that the study could consequently cover the entire transition. Corresponding dimensionless EHL parameters are G^*=4000, W^*=1.008×10^{-5} and U^*=2.298 ×10^{-17}~3.448 ×10^{-10}.

In the first set of sample cases smooth surfaces are used, as the smooth surface solution is an important reference and baseline when studying roughness effect. Also, it serves as a test for evaluating and demonstrating the validity of the numerical model described above. Figure 1 shows the results from 9 cases at different rolling speeds from 15000 mm/s down to 0.001 mm/s. The slide-to-roll ratio is fixed at S=2.0 (simple sliding condition). It can be seen that when the rolling speed is high, 2500-15000 mm/s, the contact is hydrodynamically lubricated, and the two surfaces are completely separated with a thick lubricant film. The solution demonstrates typical full film EHL characteristics, as shown in Figs.1 (a) and (b). When the rolling speed decreases, the film thickness is gradually reduced, and the pressure distribution is getting closer and closer to that of the Hertzian dry contact, as observed in Figs. 1(c), (d) and (e). If the speed is further reduced, solid-to-solid contact occurs first on the downstream side due to insufficient hydrodynamic action, as shown in Fig. 1(f). As the speed continues to go down, the contact area expands gradually to the upstream (see Figs. 1(g) and (h)), and then eventually covers the entire Hertzian contact zone. In order to test the robustness of the computer program, the extremely low speed of U=0.001 mm/s is used in the last case, and a converged solution is obtained successfully, as given in Fig. 1(i). Since the speed is nearly zero, the hydrodynamic effect vanishes, and it can be practically considered as a dry contact. The pressure distribution obtained from the unified numerical approach and the reduced Reynolds Equation is found to be in good agreement with the conventional Hertzian theory.

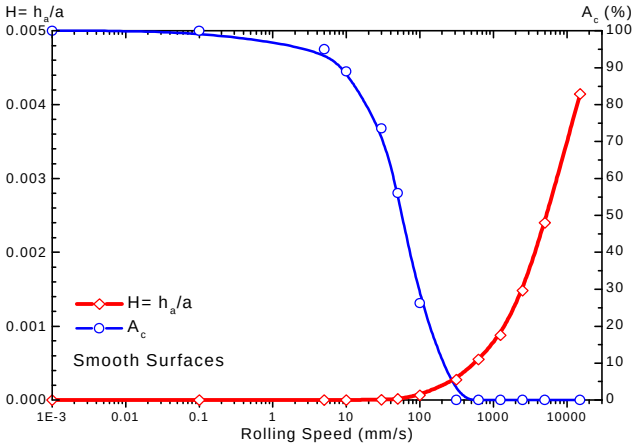

Figure 2

The results of average film thickness, h_a, and contact area ratio, A_c, vs. rolling speed for these smooth cases are plotted in Figure 2. Please note that the contact area ratio is defined as the ratio of contact area to that of nominal Hertzian contact zone. It can be seen that when the speed is higher than 300 mm/s or so, there is no solid-to-solid contact (A_c=0) and it is in the full film lubrication region. If the speed is lower than a certain limit, around 10 mm/s, the average film thickness in the center part of Hertzian contact zone becomes zero, and the contact area ratio A_c equal or close to 100%. The hydrodynamic effect is insignificant and this is actually in the boundary lubrication region. The transition zone in between can be clearly seen in the figure, where the hydrodynamic effect and the solid-to-solid contact co-exist.

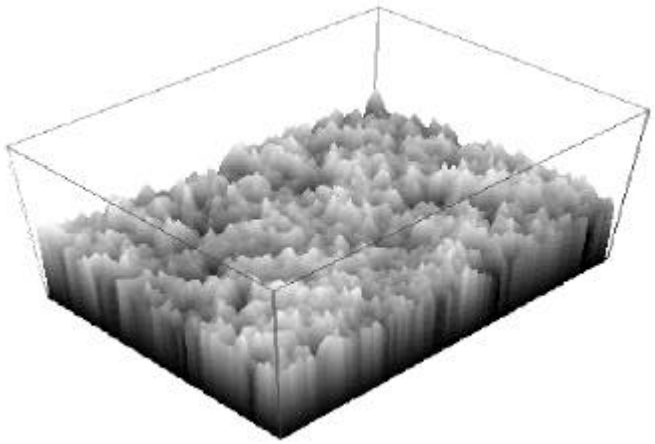

Figure 3. A Shaved Surface

A shaved surface is employed in the second set of calculation cases in order to study the transition with real 3-dimensional roughness. Optically measured topography of this shaved surface is shown in Figure 3. The RMS roughness is R_q= 0.4 μm, and the topography is found to be nearly isotropic. Since the slide-to-roll ratio is fixed at S=0.2, the solution is transient in nature due to deformed moving surface asperities. It may take 180-200 time steps to get the solution stabilized when using an initial value from a smooth surface solution under the same operating conditions. Calculation results for 9 cases at different rolling speeds are illustrated in Figure 4. The speed range is also 0.001-15000 mm/s in order to compare with the smooth surface cases presented above.

It is observed from Figs. 4(a) and (b) that when the rolling speed is very high, 15000 mm/s, the lubricant film is sufficiently thick at a λ ratio of 5.784, so that the two surfaces are completely separated. This is obviously the full film lubrication. If the speed is reduced to 2500 mm/s, the λ ratio is found to be 1.798 and this may still be considered as the full film EHL. However, there could be occasionally some slight insignificant asperity contacts, and the contact area ratio could be in the neighborhood of 1-3%. When the speed is down to 1250 mm/s, the lubricant film becomes thinner at λ=1.050, and the asperity contacts more noticeable, A_c=12.46%, as seen in Fig.4(c). If the speed continues to decrease, the average film thickness gets smaller and more severe asperity contacts are initiated, as shown in Figs. 4(d) and (e). The λ ratios are 0.610 for U=625 mm/s and 0.391 for U=312.5 mm/s, respectively. When the speed goes down to 100 mm/s, the contact area ratio is found to be about 59.99% and the λ ratio about 0.203 (see Fig. 4(f)). If the speed is further reduced, U≤30 mm/s, the hydrodynamic action is significantly reduced and more than 70% of load is supported by the asperity contacts. This may be considered as the boundary lubrication. For the extremely low speed, U=0.001 mm/s, the λ ratio is reduced down to 0.0282, and the contact area ratio about 95.0%. Please note that in the boundary lubrication region the hydrodynamic effect is generally insignificant. However, as long as the surface asperities are not completely flattened, there may still be some lubricant retained in the "pockets" formed by still-existing roughness, and a small percentage of load may still be supported by the lubricant film. The contact area ratio may not be 100% even at extremely low speeds.

In order to see the entire transition more clearly, the results of λ ratio and contact area ratio vs. rolling speed are plotted in Figure 5. It is important to note that when the speed is continuously decreasing, the solid-to-solid contact starts to take place as soon as the speed becomes lower than 2500 mm/s. It is much earlier than that for the smooth solution, 300 mm/s. This is obviously due to the existence of surface roughness. For the same average film thickness the smooth surfaces are still separated, but the rough surfaces may have already had noticeable asperity contacts initiated. On the other hand, when the

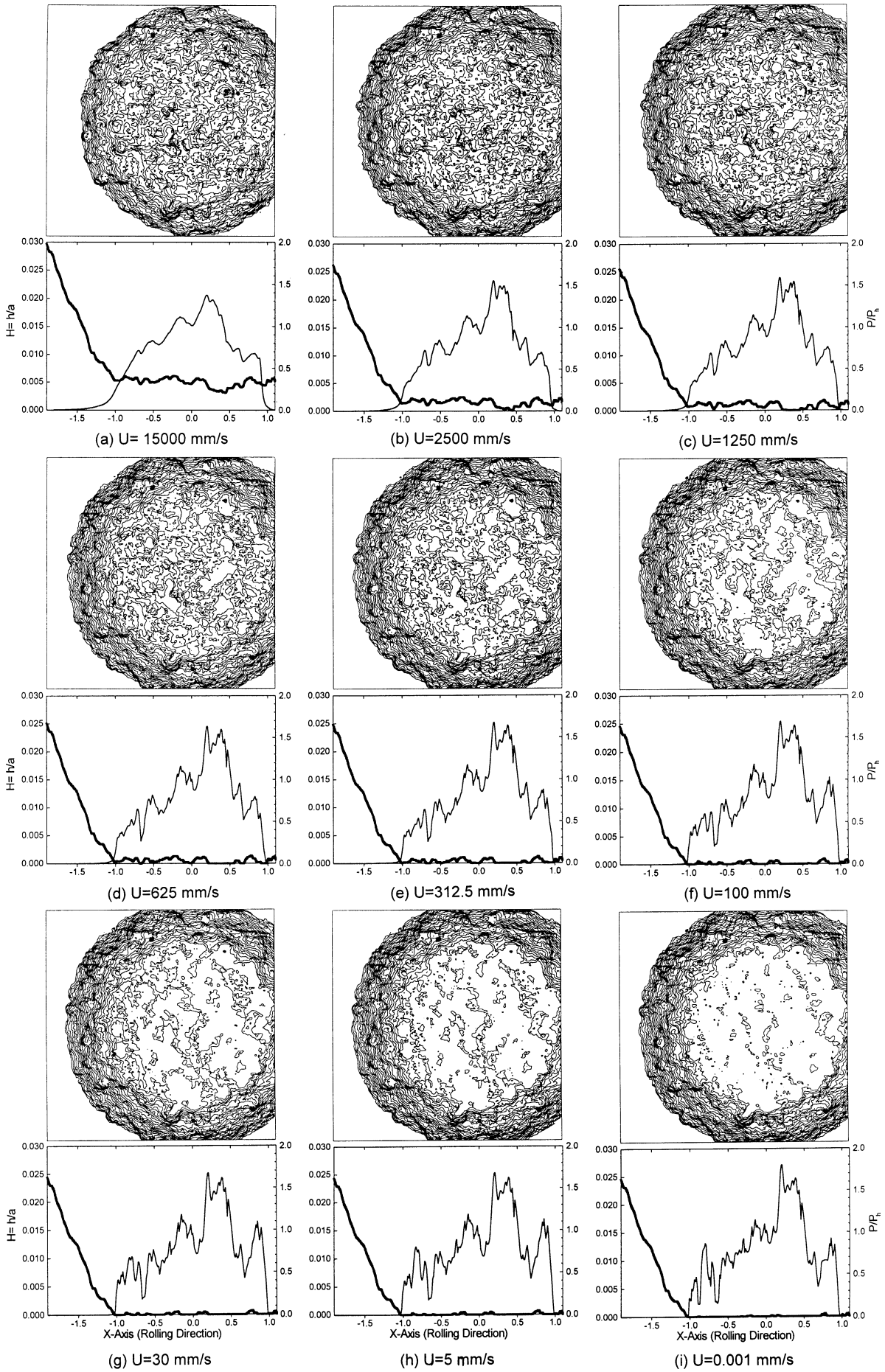

(a) U= 15000 mm/s (b) U=2500 mm/s (c) U=1250 mm/s

(d) U=625 mm/s (e) U=312.5 mm/s (f) U=100 mm/s

(g) U=30 mm/s (h) U=5 mm/s (i) U=0.001 mm/s

Figure 4

speed is in the low range, 10-30 mm/s or lower, the average film thickness for the smooth surface solution is already zero, as seen in Figure 2, but that for the rough surface solution is still noticeably larger than zero. Even at U=0.001 mm/s the λ ratio for the rough surface solution is not zero. This is because the surface roughness is very helpful to retain lubricant in the contact zone, and the squeeze effect caused by the rolling movement and the retained lubricant would positively affect the lubricant film formation.

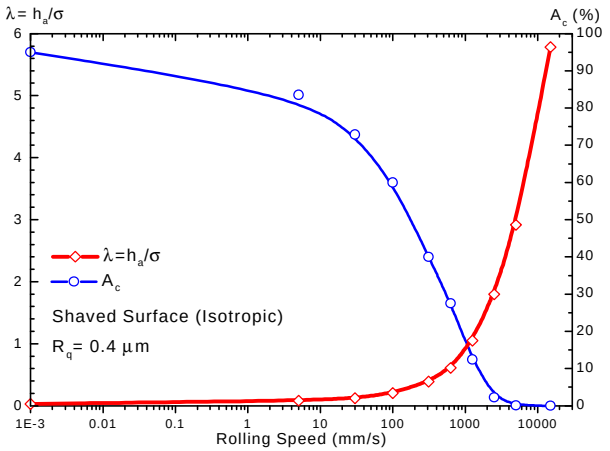

Figure 5

Figure 6 shows the area sharing between the hydrodynamic and contact regions as a function of λ ratio based on the results from the shaved surface. For comparison purposes, the load sharing is also plotted in the figure. It can be seen that the load sharing is directly correlated with the area sharing, but they may be slightly different in quantity. When the λ ratio is small, the percentage of hydrodynamic load could be slightly larger than that of hydrodynamic area due to the relatively more significant squeeze effect caused by the retained lubricant in the rough surface contact zone.

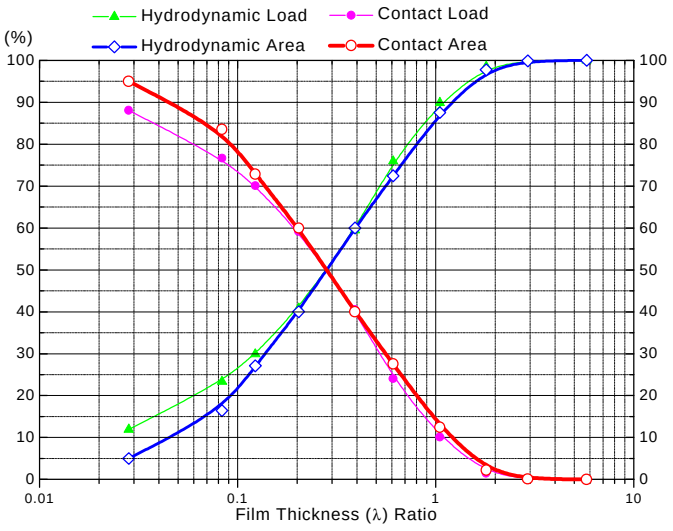

Figure 6 (Shaved Surface, R_q=0.4 μm)

CONCLUSIONS

The calculation results presented above have demonstrated that the new numerical approach developed in the present study is simple and robust, capable of solving lubrication and contact problems for commonly used machined surfaces with 3-dimensional roughness under very severe operating conditions. Full numerical solutions can be achieved with a unified numerical procedure, simulating the entire transition from the full film, mixed, down to boundary lubrication. So far no convergence problem has been encountered in the analyzed cases that cover a full range of λ ratio from infinity down to nearly zero (less than 0.03). Evidently, the computer program developed can be a useful engineering tool for analyzing/predicting rough surface lubrication and contact characteristics as well as surface failure mechanisms in gears, bearings, cams, traction drives and other mechanical components used in various industrial applications.

ACKNOWLEDGMENTS

The authors would like to express their appreciation for the continuous support by Mr. John Bair and Mr. Rich Nellums of Eaton Corporation. Dr. Xiaolan Ai of Timken Company should also be acknowledged for his input in discussion during the early stage of this study.

REFERENCES

(1) Christensen, H., "Stochastic Models for Hydrodynamic Lubrication of Rough Surfaces," Proc. Instn. Mech. Engrs., Vol. 184, Part 1, No. 55, pp.1013-1026 (1969-70).

(2) Elrod, H. G., "Thin-Film Lubrication Theory for Newtonian Fluids Possessing Striated Roughness or Grooving," ASME Journal of Lubrication Technology, Vol. 93, pp. 324-330 (1973).

(3) Tonder, K., "Mathematical Verification of the Applicability of Modified Reynolds Equation to Striated Rough Surfaces," Wear, Vol. 44, No. 2, pp.329-343 (1977).

(4) Patir, N., and Cheng, H.S., "An Average Flow Model for Determining Effects of Three- Dimensional Roughness on Partial Hydrodynamic Lubrication," ASME Journal of Lubrication Technology, Vol.100, pp.12-17 (1978).

(5) Zhu, D., and Cheng, H.S., "Effect of Surface Roughness on the Point Contact EHL," ASME Journal of Tribology, Vol.110, pp.32-37 (1988).

(6) Lubrecht, A. A., ten Napel, W. E., and Bosma, R., "The Influence of Longitudinal and Transverse Roughness on the Elastohydrodynamic Lubrication of Circular Contacts," ASME Journal of Tribology, Vol. 110, pp. 421-426 (1988).

(7) Kweh, C. C., Evans, H. P., and Sindle, R. W., "Micro-Elastohydrodynamic Lubrication of An Elliptical Contact with Transverse and 3-Dimensional Roughness," ASME Journal of Tribology, Vol. 111, pp.577-584 (1989).

(8) Kweh, C. C., Patchong, M. J., Evans, H. P. and Snidle, R. W., "Simulation of Elastohydrodynamic Contacts Between Rough Surfaces," ASME Journal of Tribology, Vol.114, pp.412-419 (1992).

(9) Ai, X., and Cheng, H.S., "The effects of Surface Texture on EHL Point Contacts," ASME Journal of Tribology, Vol.118, pp.59-66 (1996).

(10) Ai, X., Cheng, H.S., and Zheng, L., "A Transient Model for Micro-Elastohydrodynamic Lubrication with 3-Dimensional Irregularities," ASME Journal of Tribology, Vol.115, pp.102-110 (1993).

(11) Ai, X., and Cheng, H.S., "The Influence of Moving Dent on Point EHL Contacts," Tribology Transactions, Vol.37, pp.323-335 (1994).

(12) Venner, C. H., and Lubrecht, A.A., "Numerical Analysis of the Influence of Waviness on the Film Thickness of a Circular EHL Contact," ASME Journal of Tribology, Vol.118, pp.153-161 (1996).

(13) Xu, G., and Sadeghi, F., "Thermal EHL Analysis of Circular Contacts With Measured Surface Roughness," ASME Journal of Tribology, Vol.118, pp.473-483 (1996).

(14) Zhu, D., and Ai, X., "Point Contact EHL Based on Optically Measured 3-Dimensional Rough Surfaces," ASME Journal of Tribology, Vol.119, pp.375-384 (1997).

(15) Jiang, X., Hua, D.Y., Cheng, H.S., Ai, X., and Lee, S.C., "A Mixed Elastohydrodynamic Lubrication Model With Asperity Contact," ASME Journal of Tribology, Vol.121, No.3 (1999).

(16) Yang, P., and Wen, S., "A Generalized Reynolds Equation for Non-Newtonian Thermal Elastohydrodynamic Lubrication," ASME Journal of Tribology, Vol.112, pp.631-636 (1990).

(17) Ai, X., " Numerical Analyses of Elastohydrodynamically Lubricated Line and Point Contacts with Rough Surfaces By Using Semi-system and Multigrid Methods," Ph. D. Dissertation, Northwestern University, Evanston, Illinois, USA (1993).